Competition for light in forest population dynamics: from computer simulator to mathematical model

Pierre Magal and Zhengyang Zhang *

Univ. Bordeaux, IMB, UMR 5251, F-33400 Talence, France

CNRS, IMB, UMR 5251, F-33400 Talence, France.

February 14, 2017

Abstract

In this article we build a mathematical model for forest growth and we compare this model with a computer forest simulator named SORTIE. The main ingredient taken into account in both models is the competition for light between trees. The parameters of the mathematical model are estimated by using SORTIE model, when the parameter values of SORTIE model correspond to the ones previously evaluated for the Great Mountain Forest in USA. We see that the best fit of the parameters of the mathematical model is obtained when the competition for light influences only the growth rate of trees. We construct a size structured population dynamics model with one and two species and with spatial structure.

Keywords: Computer forest simulator, SORTIE model, size structured model, spatial structured model, state dependent delay differential equations.

Manuscript type: Article.

*This author is supported by Chinese Scholarship Council (CSC).

Introduction

In the natural ecosystem, forests play an important role. This has motivated a lot of people to propose computer simulators as well as mathematical models to describe the dynamical properties of forests. Many computer simulators (also sometimes called Individual Based Models (IBMs)) have been proposed and we refer to JABOWA [3, 4], FORET [35], SORTIE [28], FORMIND [14] and others. These models consist of stochastic processes describing individual behaviors, such as birth, death, movement, reproduction and so on. Moreover, these models also permit us to describe the behavior of the entire plant community. The main advantage is that it provides simulated data which can be used to analyze such a complex system. Of course this is a rough description of the real plant community. However, they do supply powerful experimental tools and describe the forest dynamics reasonably well [20]. We refer to [21, 30] for a general review about forest IBMs.

SORTIE is a forest simulator based on the forest data observed in and around Great Mountain Forest (GMF), a privately owned 2500ha forest located in northwestern Connecticut (41°57'N, 73°15'W), USA in the year 1990-1992. In SORTIE, four submodels (resource, growth, mortality, and recruitment) are included to determine the behaviour of each individual. As is explained in [27], from the point of view of the resource competition, SORTIE includes only the light competition, since from extra experiments very little evidence of water or nitrogen limitation has been observed for this particular forest. Nevertheless water or nitrogen limitation might be vital in other forests. The lighting mechanism in SORTIE is rather complex and we refer to the subsection *Resource submodel* page 3 in [27] for more about this. Tree growth is described by change of tree size, which is denoted here as the diameter at a certain height. Two concepts "diam_{10} (Diameter at 10cm Height)" and "DBH (Diameter at Breast Height)" are often used to describe the tree growth and represent the tree size in the analysis of forest dynamics [27, 28, 32]. Thereinto, the diam_{10} can be used almost throughout the whole life of an individual, from seedling to adult, while DBH can only be used for adults in most cases, as it is measured at

a higher height. The definition of the breast height (of an adult human being) is different in different regions, for example, 1.4m in the US and 1.3m in Europe and Canada. But it makes little difference to the measuring result in many cases. We refer to [13, 27, 28, 29, 32, 40] for more details of SORTIE.

In this article we will extend the model proposed by Hal Smith in [37, 38] to describe the dynamic of a population that is structured in size with intra-specific competition for light. For a single species, we will compare such a mathematical model with SORTIE model for two types of tree (American beech (FAGR) and eastern hemlock (TSCA)). The reason why we choose particularly these two types of tree is that after a tentative run of SORTIE, we find that FAGR and TSCA dominates the forest in an obvious way (see Figure 1). Moreover, based on the parameters estimated separately for each kind of tree, we will investigate the inter-specific competition for light by assuming that the growth rate of juveniles is influenced by the number of adults due to the competition for light between them. We will also extend our modelling effort by considering the case of two populations distributed in space and competing for light.

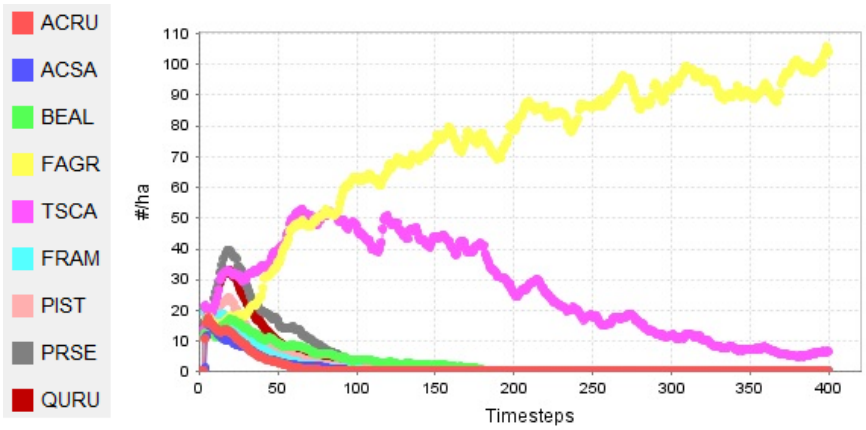

Figure 1: *The output of one run of SORTIE for all the nine species on a period of 2000 years (1 time step=5 years).*

Several mathematical models describing the forest growth were proposed in the literature. Zavala et al. [44] studied a stage-structured population model incorporating the light competi-

tion respectively in growth, mortality and recruitment, and gave the conditions for the existence of a steady state distribution. Angulo et al. [2] continued with a similar model, but they considered the light competition only in recruitment, and after that they extended the model to a two-species stand, and gave the positive stationary distribution for both single-species and two-species model and the conditions for the coexistence. Cammarano [5] studied a system of Lotka-Volterra type, incorporating also the light competition and discussed the equilibria and the coexistence conditions. In this article, based on SORTIE simulated data, we will exclude the competition occurring in the mortality and recruitment. In other words, we will see that the best fit for SORTIE model is obtained by using a model where the competition for light influences only the growth rate of trees. We also refer to [7, 12, 15, 17, 25, 39, 43] and the references therein for other models and relevant researches.

The article is organized as follows. In section 2 we will give a mathematical model for single species, and we will conduct numerical simulations to compare with SORTIE. In section 3 a mathematical model for two species is obtained likewise, and we also conduct the comparison with SORTIE. Then in section 4 we extend it to a 2-dimension spatial model, and conduct numerical simulations to see the spread of trees in space.

Single species model

Mathematical modelling

In this section we consider the following model describing the growth of trees of single species

$$\begin{cases} \partial_t u(t,s) + \underbrace{f(A(t))\partial_s u(t,s)}_{\text{growth of trees}} = -\underbrace{\mu(s)}_{\text{mortality}} u(t,s), \text{ for } t>0, s>s_-, \\ f(A(t))u(t,s_-) = \underbrace{\beta b(A(t))}_{\text{flux of newborns}}, \text{ for } t>0, \\ u(0,.) = u_0(.) \in L^1(s_-,+\infty). \end{cases} \tag{0.1}$$

Here $u(t,s)$ denotes the population density of trees with size s at time t, so $\int_{s_1}^{s_2} u(t,s)ds$ is the number of trees with size $s \in [s_1, s_2]$ at time t, and $A(t)$ is the number of adult population at time t. As it will be explained in Appendix A, the size s is described by a function of diam_{10}

$$s(t) := \ln \frac{r(t)}{r_-}, \text{ and } r(t) = \frac{\text{diam}_{10}(t)}{2}$$

where r_- is the minimal radius of the juvenile. The function $\mu(s) > 0$ is the natural mortality. In the following derivation we will assume for simplicity that

$$\mu(s) = \begin{cases} \mu_A > 0, \text{ if } s \geqslant s^*, \\ \mu_J > 0, \text{ if } s \in [s_-, s^*), \end{cases}$$

where $s_- > 0$ is the minimal size of a juvenile and s^* satisfying $s^* > s_-$ is the maximal size of a juvenile (or the minimal size of an adult). The parameter β is the birth rate in absence of birth limitation, and the term $\beta b(A(t))$ describes the flux of newborns into the population, where $b(x) = xe^{-\xi x}$ is the Ricker's type birth limitation [33, 34]. The growth function $f(x)$ takes the form

$$f(x) = \frac{\alpha}{1+\delta x}, \ \alpha, \delta > 0, \tag{0.2}$$

which is decreasing, thus taking care of the fact that the more large trees there are, the slower the growth rate of small trees is. So this shows the type of competition for light between adults and juveniles. The function $u_0(.)$ represents the initial distribution of the species. Normally we want the number of the total population to be finite at each time, hence we have

$$\int_{s_-}^{+\infty} u(t,s)ds < +\infty, \ \forall t \geqslant 0.$$

So the natural state space for this model is $L^1(s_-, +\infty)$.

We will derive the following equations for adults and juveniles under some assumptions

$$\begin{cases} \dfrac{dA(t)}{dt} = f(A(t))j(t,s^*) - \mu_A A(t), \text{ for } t > 0, \\ \partial_t j(t,s) + f(A(t))\partial_s j(t,s) = -\mu_J j(t,s), \text{ for } s \in [s_-, s^*), t > 0, \\ f(A(t))j(t,s_-) = \beta b(A(t)), \text{ for } t > 0, \\ A(0) = A_0 \geqslant 0, \\ j(0,s) = j_0(s) \geqslant 0, \text{ for } s \in [s_-, s^*), \end{cases} \tag{0.3}$$

where $j(t,s)$ represents the population density of juveniles with size $s \in [s_-, s^*)$ at time t. Hence the total number of juveniles at time t is

$$J(t) = \int_{s_-}^{s^*} j(t,s)ds = \int_{s_-}^{s^*} u(t,s)ds.$$

And we can assume as follows the adult population number

$$A(t) = \int_{s^*}^{+\infty} u(t,s)ds. \tag{0.4}$$

By integrating along the characteristic line of the second equation (of juvenile) in (0.3), the first equation (of adult) in (0.3) can be rewritten as the following state dependent Functional Differential Equation (FDE)

$$\begin{cases} \dfrac{dA(t)}{dt} = e^{-\mu_J \tau(t)} \dfrac{f(A(t))}{f(A(t-\tau(t)))} \beta b(A(t-\tau(t))) - \mu_A A(t), \\ \displaystyle\int_{t-\tau(t)}^{t} f(A(\sigma))d\sigma = s^* - s_- \end{cases} \tag{0.5}$$

when $t > t^*$, where t^* is defined as

$$\int_0^{t^*} f(A(\sigma))d\sigma = s^* - s_-.$$

Differentiation of the second equation with respect to t gives the following system

$$\begin{cases} A'(t) = e^{-\mu_J \tau(t)} \dfrac{f(A(t))}{f(A(t-\tau(t)))} \beta b(A(t-\tau(t))) - \mu_A A(t), \\ \tau'(t) = 1 - \dfrac{f(A(t))}{f(A(t-\tau(t)))}. \end{cases} \tag{0.6}$$

The initial conditions are

$$A(t) = A_0(t) \geqslant 0, \forall t \in (-\infty, 0];\ \tau(0) = \tau_0 \geqslant 0, \tag{0.7}$$

where $A_0(t)$ is continuous and exponentially bounded, namely for some $\vartheta > 0$

$$\sup_{t\leqslant 0} e^{\vartheta t} A_0(t) < +\infty.$$

From the second equation of (0.5), as f is decreasing, the delay $\tau(t)$ can become large enough, namely we may have infinite delay. For all the derivation here, see Appendix A. The semiflow properties of such a state-dependent delay differential equation will be studied in [24].

Numerical simulations of two special cases

We conduct numerical simulations for two special cases of the system (0.5).

Special case 1 ($f(x)$ is constant): Assume that $f(x)$ is a constant function (so the delay $\tau(t)$ is also constant by the second equation of (0.5)) and $b(x) = xe^{-x}$. Then since the PDE model (0.1) can be transformed (by making a simple change of variable in time) into an age structured model, it is known (see Magal and Ruan [23]) that the system has a Hopf bifurcation around the positive equilibrium when β increases (see in Figure 2).

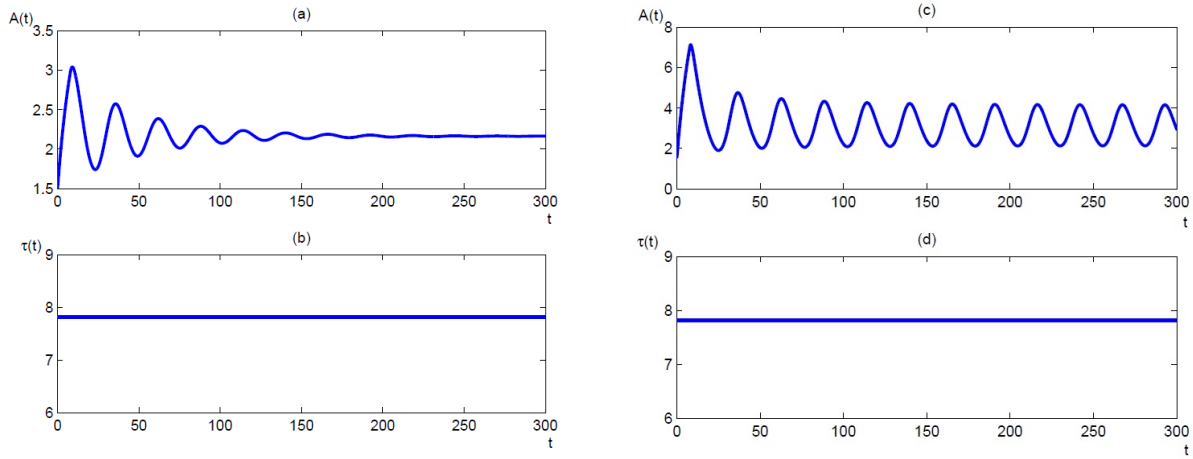

Figure 2: *We plot the adult population number $A(t)$ in figure (a) and (c), and the corresponding delay $\tau(t)$ in figure (b) and (d). We fix the parameter values $\mu_J = 0.2$, $\mu_A = 0.1$, $\alpha = 0.5$, $\delta = 0$, $\xi = 1$, $s^* = \ln 50$, $s_- = 0$, and the initial distribution $A_0(t) = 1.5$, $\forall t \in [-100, 0]$. In (a) and (b) we set $\beta = 9$. The solution oscillates and then converges to the positive equilibrium. In (c) and (d) we set $\beta = 25$. Changing β from 9 to 25, we observe a Hopf bifurcation.*

Special case 2 ($b(x) = x$): Assume $b(x) = x$, namely the Ricker's type birth function doesn't appear in system (0.5). It is known that when τ is constant in the first equation (which becomes linear) of system (0.5), this system is either exponentially increasing or exponentially decreasing when the time goes to infinity. However, it has been proved by Smith [37] that Hopf bifurcation can occur when we take state-dependent delay. This is illustrated in Figure 3.

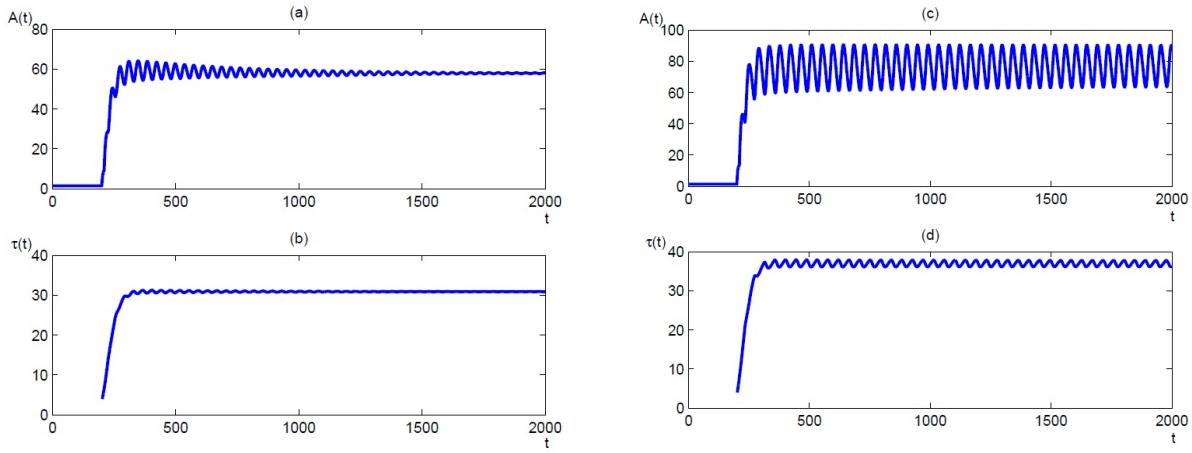

Figure 3: *We plot the adult population number $A(t)$ in figure (a) and (c), and the corresponding delay $\tau(t)$ in figure (b) and (d). We fix the parameter values $\mu_J = \mu_A = 0.1$, $\delta = 0.1$, $\xi = 0$ (remember this means that $b(x) = x$), and the initial delay $\tau_0 = 4$. The initial distribution is $A_0(t) = 1.5$, $\forall t \in [0, 200]$. In (a) and (b) we set $\beta = 2.2$, then we have the damped oscillating solution which converges to the positive equilibrium; In (c) and (d) we set $\beta = 4$. Changing β from 2.2 to 4, we observe a Hopf bifurcation.*

Comparison with SORTIE

We run the simulator SORTIE with the parameter values given in [13, 28, 32, 40] and get the simulation for the density of adult trees (adults are defined here as trees having a DBH $\geqslant$ 10cm). And as we can see from this simulation, American beech(FAGR) and eastern hemlock(TSCA) become the dominant species after a period time. So in this article we will focus on these two species in two cases: one single species and two-species.

The basic idea of the numerical simulation of (0.5) and comparison is as follows. Before starting, we need to get the forest data from SORTIE. Since every run of SORTIE is initiated with

a random seed, we conduct 50 runs and take the average values as our actual data. Moreover, the data that SORTIE gives are actually the density of the adult population per hectare. As the area of the sample square is 90000m^2 (a square of 300m$\times$300m) = 9 hectares, we multiply the data by 9 to obtain the total adult population number. We plot the 50 runs and the average in Figure 4 to see the stochastic variation.

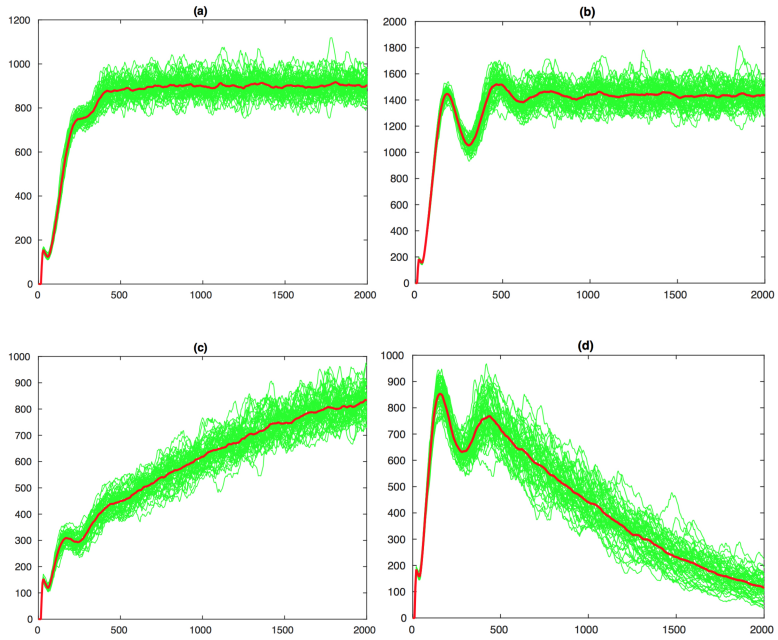

Figure 4: *Population numbers of 50 random runs from SORTIE for the adults of two species American beech and eastern hemlock(green curve) and the average number(red curve) respectively, in a period of 400 timesteps. (a). One single species American beech; (b). One single species eastern hemlock; (c). Two-species case: American beech; (d). Two-species case: eastern hemlock.*

Now we will compare our model (0.5) with the mean value over these 50 runs of SORTIE, and find the best fit. First we need to decide the initial time (for example, $t = 100$ as the initial time), and we will use the data from SORTIE over the time interval $[0, 100]$ as the initial condition. Next we discretize the parameters $\mu_J, \mu_A, \beta, \xi, \delta, \tau_0$, and for each set of parameters, we calculate the solution of (0.5) by using the common approximation of the derivative (the numerical scheme will be conducted via the equivalent system (0.6)), and we compare the numerical solutions with

the data from SORTIE by using the least square method, to find the set of parameter values with which the numerical result of the model (0.5) and the data have the least difference. Then we use the following formula (see Appendix A)

$$\int_{-\tau_0}^{0} \frac{\alpha}{1+\delta A(\sigma)} d\sigma = s^* - s_-,$$

to compute α, where we use the Simpson's rule to calculate the integral. Now we can keep this set of parameter values, and we have the best fit to SORTIE.

For the first dominant species American beech, we choose the SORTIE data in the time interval [0,200] as the initial distribution. We have the best fit in Table 1 and Figure 5.

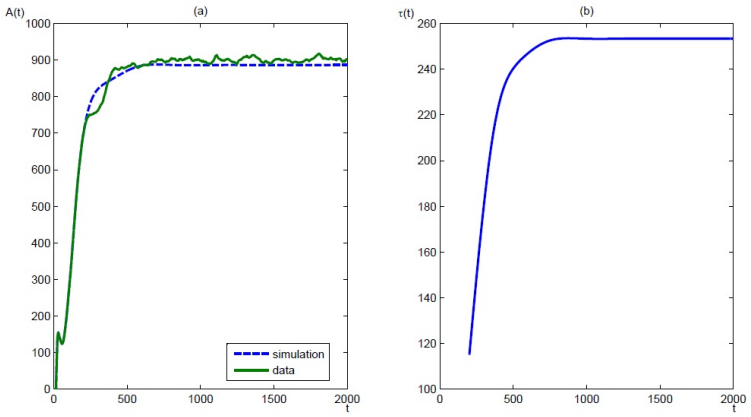

Figure 5: *In this figure we show the comparison between SORTIE data and numerical simulation for American beech. The adult population number $A(t)$ is plotted in (a) and the delay $\tau(t)$ is shown in (b).*

Similarly, for the second dominant species eastern hemlock we choose the SORTIE data in the time interval [0,180] as the initial distribution. We get the best fit in Table 2 and Figure 6.

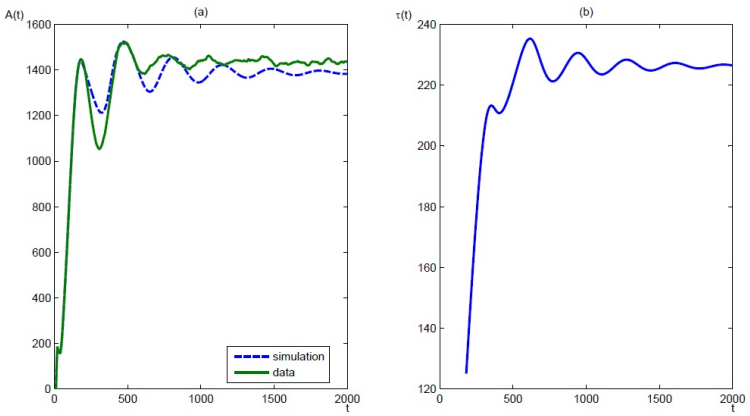

Figure 6: *In this figure we show the comparison between SORTIE data and numerical simulation for eastern hemlock. The adult population number $A(t)$ is plotted in (a) and the delay $\tau(t)$ is shown in (b). Notice that this species will have an oscillation before it converges to the stable positive equilibrium.*

Notice that for both species in the single species case, we have $\xi_1 = \xi_2 = 0$ as the best fit, which means that there is no Ricker's type birth limitation here.

Two-species model

Mathematical modelling

System (0.1) can be extended to the case of two species. Taking the previous best fit $\xi_1 = \xi_2 = 0$ into account, we obtain the following system

$$\begin{cases} \partial_t u_1(t,s) + f_1(Z_1(t))\partial_s u_1(t,s) = -\mu_1(s)u_1(t,s), \text{ for } t > 0, s > s_-, \\ \partial_t u_2(t,s) + f_2(Z_2(t))\partial_s u_2(t,s) = -\mu_2(s)u_2(t,s), \text{ for } t > 0, s > s_-, \\ f_1(Z_1(t))u_1(t,s_-) = \beta_1 A_1(t), \text{ for } t > 0, \\ f_2(Z_2(t))u_2(t,s_-) = \beta_2 A_2(t), \text{ for } t > 0, \\ u_1(0,\cdot) = u_{10}(\cdot) \in L^1(s_-, +\infty), \\ u_2(0,\cdot) = u_{20}(\cdot) \in L^1(s_-, +\infty), \end{cases} \tag{0.8}$$

where

$$Z_i(t) = \zeta_{i1}A_1(t) + \zeta_{i2}A_2(t),\ f_i(x) = \frac{\alpha_i}{1+\delta_i x},\ \mu_i(s) = \begin{cases} \mu_{A_i} > 0, & \text{if } s \geqslant s^*, \\ \mu_{J_i} > 0, & \text{if } s \in [s_-, s^*), \end{cases}$$

and $\zeta_{ij} \geqslant 0$ are non-negative constants, $\alpha_i, \delta_i > 0$, $i, j = 1, 2$. A specific explanation of the meaning of ζ_{ij} can be found in Table 3. Notice that we use the same minimal juvenile size s_- and minimal adult size s^* for both species (see [27]). After a similar derivation, we have the following state-dependent delay differential equations

$$\begin{cases} A_i'(t) = e^{-\mu_{J_i}\tau_i(t)} \dfrac{f_i(Z_i(t))}{f_i(Z_i(t-\tau_i(t)))}\beta_i A_i(t-\tau_i(t)) - \mu_{A_i}A_i(t), \\ \displaystyle\int_{t-\tau_i(t)}^{t} f_i(Z_i(t))d\sigma = s^* - s_-, \end{cases} \tag{0.9}$$

$i = 1, 2$. We give the following expression for the sake of numerical simulation

$$\begin{cases} A_i'(t) = e^{-\mu_{J_i}\tau_i(t)} \dfrac{f_i(Z_i(t))}{f_i(Z_i(t-\tau_i(t)))}\beta_i A_i(t-\tau_i(t)) - \mu_{A_i}A_i(t), \\ \tau_i'(t) = 1 - \dfrac{f_i(Z_i(t))}{f_i(Z_i(t-\tau_i(t)))}. \end{cases} \tag{0.10}$$

Comparison with SORTIE

We use the same method of comparison as before and we use the parameters in Table 1 and Table 2 to simulate the two-species model. We discretize the new parameters ζ_{ij} appeared in the competition term, and also by the least square method, we get the best fit for them: $\zeta_{11} = 1$, $\zeta_{12} = 0.6$, $\zeta_{21} = 1.6$, $\zeta_{22} = 1$, and the delay τ_{01} is increased to 201, τ_{02} increased to 208. We list these values in Table 3. The comparison figure is in Figure 7.

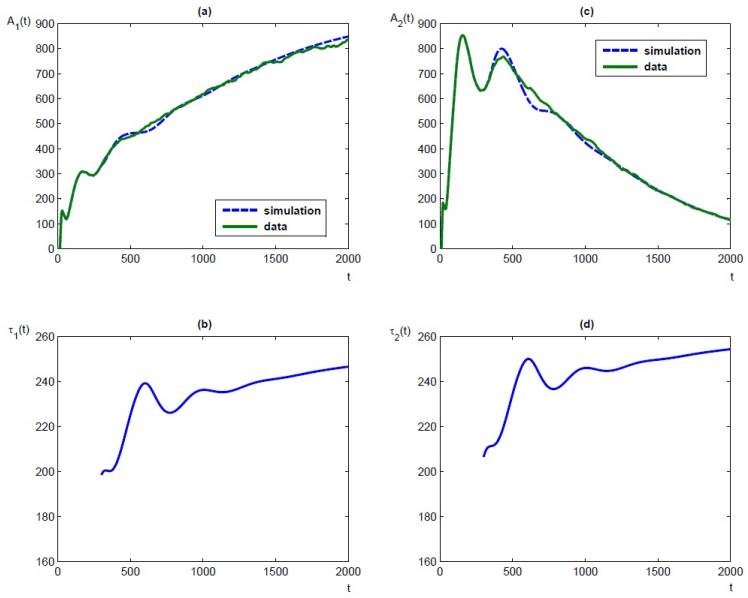

Figure 7: *In this figure we plot the comparison between SORTIE data and numerical simulation for two-species model (0.9). The figures (a) and (c) show the adult population number for species 1 American beech and species 2 eastern hemlock respectively. The figures (b) and (d) show the corresponding time delay.*

By analyzing the existence positive (coexisting) equilibrium (see Appendix B), we can also obtain the coexistence of both American beech and eastern hemlock in Figure 8.

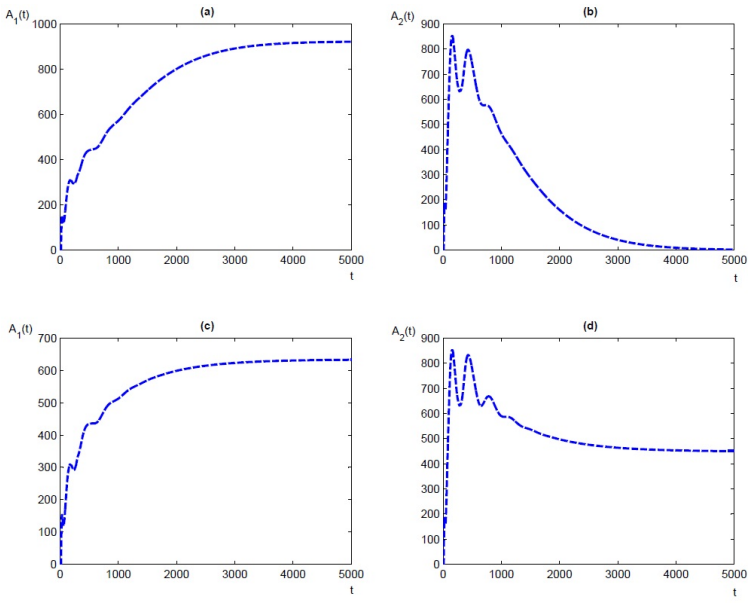

Figure 8: *In this figure we demonstrate that we can pass from competitive exclusion (a)(b)(which corresponds to Figure 7) to coexistence (c)(d) by changing one parameter* ζ_{21}*. The other parameters are the same as in Figure 7. When* $\zeta_{21} = 1.6$*, American beech (a) reaches to a positive steady state while eastern hemlock (b) disappears gradually. After we decrease the value of* ζ_{21} *to* 1*, both American beech (c) and eastern hemlock (d) go to a positive steady state, which means coexistence.*

Two-species spatial model

Now we take the spatial position of the individuals into account to see the spread of the adult population. We assume that the diffusion of individuals is due to the spreading of seeds around the trunk. This corresponds to assume that the distribution of seeds, when they fall down around the trunk, follows a Gaussian distribution. The same idea has already been proposed by Ducrot [10]. The spatial model with two species reads as follows

$$
\begin{cases}
\partial_t u_i(t,s,x,y) + f_i(Z_i(t,x,y))\partial_s u_i(t,s,x,y) = -\mu_i(s)u_i(t,s,x,y), \\
\qquad\qquad\qquad\qquad \text{for } t>0, s>s_-, x\in[0,x_{\max}], y\in[0,y_{\max}], \\
f_i(Z_i(t,x,y))u_i(t,s_-,x,y) = (I-\varepsilon_i\Delta)^{-1}(\beta_i A_i(t,.,.))(x,y), \\
\qquad\qquad\qquad\qquad \text{for } t>0, x\in[0,x_{\max}], y\in[0,y_{\max}], \\
u_i(t,x,0) = u_i(t,x,y_{\max}),\ \text{for } x\in[0,x_{\max}], \\
u_i(t,0,y) = u_i(t,x_{\max},y),\ \text{for } y\in[0,y_{\max}], \\
u_i(0,s,x,y) = u_{i0}(s,x,y) \in L^1((s_-,+\infty)\times[0,x_{\max}]\times[0,y_{\max}]),
\end{cases}
\tag{0.11}
$$

where

$$
Z_i(t,x,y) = \zeta_{i1}A_1(t,x,y) + \zeta_{i2}A_2(t,x,y), f_i(x) = \frac{\alpha_i}{1+\delta_i x},
$$

$\zeta_{ij} \geqslant 0$, $\alpha_i, \delta_i > 0$, $i = 1,2$, and Δ is the Laplacian operator with periodic boundary condition. Similarly, we assume the adult population number

$$
A_i(t,x,y) = \int_{s^*}^{+\infty} u_i(t,s,x,y)ds, i = 1,2,
$$

and by following a similar procedure as before, we get the state-dependent delay differential equation for the adult

$$
\begin{cases}
\dfrac{\partial A_i(t,x,y)}{\partial t} = e^{-\mu_{I_i}\tau_i(t,x,y)}\dfrac{f_i(Z_i(t,x,y))}{f_i(Z_i(t-\tau_i(t,x,y),x,y))}(I-\varepsilon_i\Delta)^{-1}[\beta_i A_i(t- \\
\qquad\qquad \tau_i(t,x,y),.,.)](x,y) - \mu_{A_i}A_i(t,x,y),\ \text{for } t>t^*, \\
\displaystyle\int_{t-\tau_i(t,x,y)}^{t} f_i(Z_i(\sigma,x,y))d\sigma = s^* - s_-,\ \text{for } t>t^*.
\end{cases}
\tag{0.12}
$$

We conduct numerical simulations for system (0.12), using the parameters in Table 1-3, and setting the diffusion coefficient $\varepsilon_1 = 0.01$, $\varepsilon_2 = 0.005$, in order to observe the growth and spread of adult population of the two species. The simulation is conducted in a $300 * 300$ square of the $x-y$ plane, as in the reference [27]. We choose the square $[0,300]\times[0,300]$ for simplicity. We use a random initial distribution $A_i(0,x,y)$ defined as follows for both species: first we discretize the interval $[0,300]$, then we choose 25 random points in the square by taking randomly 5 points on x-axis and y-axis respectively and we assign a non-zero random number to each of the 25 points

as the population number of adults $A_i(0, x, y)$. For the rest discretized points in the square, we assign 0 to them.

Next we plot the solutions of system (0.12) at several specified time in Figure 9. The x- and y-axis describe the spatial coordinates, and the z-axis is the adult population number. In this figure we will observe the growth of the two species and the spread in space, and we can also see vividly that the model generates obvious species isolates after some time.

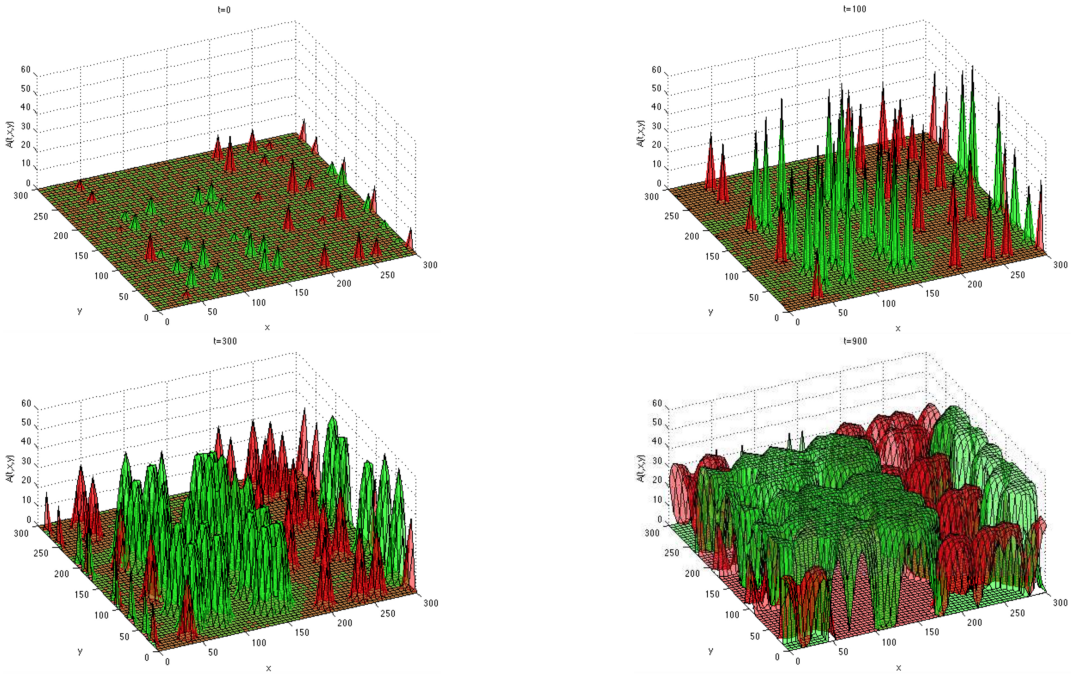

Figure 9: *In this figure we show the numerical simulations for the spatial model (0.12), describing the spread of adult population of the two species. The red part represents species 1 American beech, and the green part represents species 2 eastern hemlock.*

We also conduct the simulation for longer time, and we get the following results in Figure 10.

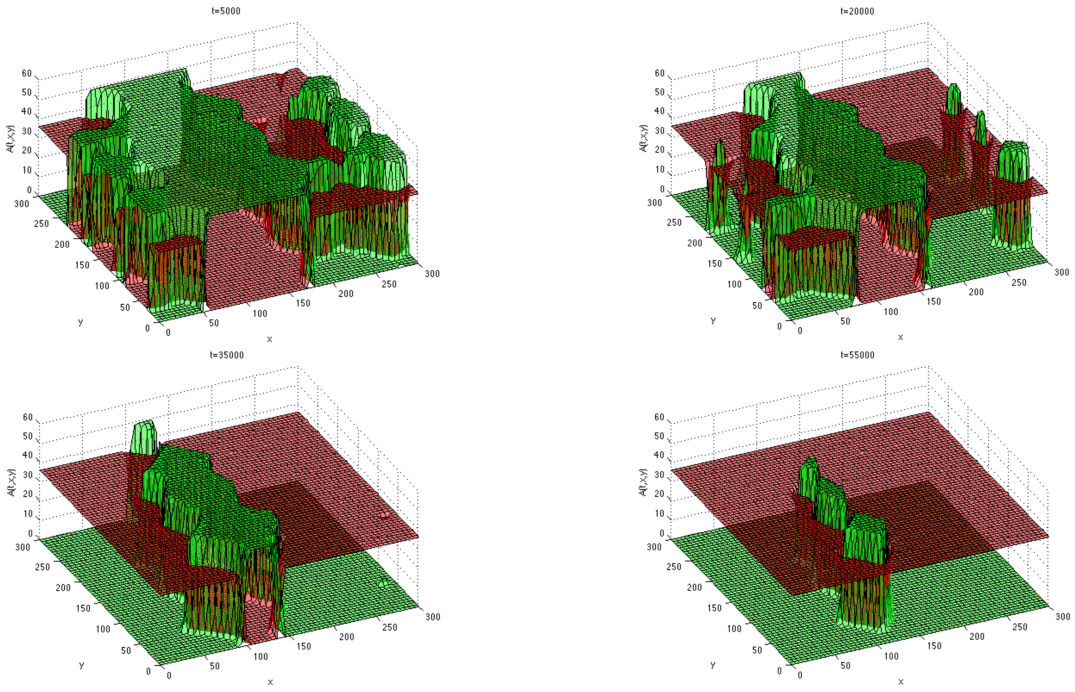

Figure 10: *This figure shows the change of the distribution of adult population of two species in the long run. Notice that eastern hemlock(green) is disappearing and American beech(red) becomes dominant.*

Summarizing all the figures above, we may conclude that eastern hemlock(green) grows and spreads faster than American beech(red) at first, but after long enough time, American beech begins to show its competency and gradually becomes the dominant species. This result also coincides with our previous result without considering the space in Figure 7.

Moreover, we plot the total population in the sample square for each species with respect to time in Figure 11. And we can see that the total adult population for eastern hemlock increases faster than American beech at first, and then it decreases.

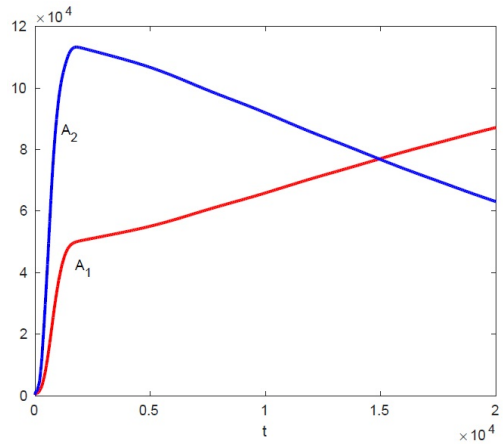

Figure 11: *In this figure we show the total population in the* $300m \times 300m$ *square for each species in 20000 years.* A_1 *represents species 1 American beech, and* A_2 *represents species 2 eastern hemlock.*

As in Figure 8, we can also observe the coexistence of both species in the spatial model. In Figure 12 we plot the long term distributions after the same change of parameters as in Figure 8.

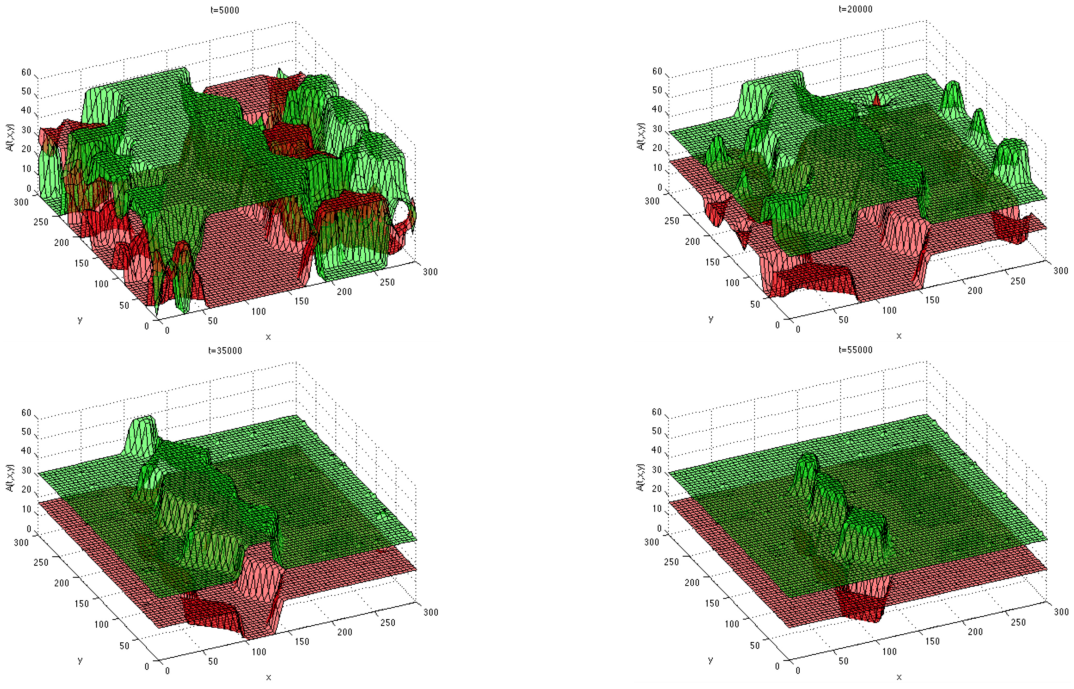

Figure 12: *The longterm simulation for the spatial model with a change of the parameter* ζ_{21} *from* 1.6 *to* 1. *All the other parameters are the same as in Figure 10. We observe the coexistence of both species.*

Discussion

Studies of forest dynamics have a long history[3, 8, 26, 31, 36]. There have been a large amount of researches on either the descriptive model (consisting of several submodels to describe separately every process of the whole life of individuals) for forests reached by observed data, or the pure mathematical model with numerical computations, separated from data. Here we first construct a mathematical model and compare this model to the computer forest simulator SORTIE. Size-structured model with another type of growth function have been previously used by Strigul et al. [39] for a single species.

We start by fitting the parameters of the model by considering the case of a single species. Then for two species, we only fit the parameters corresponding to the competition for light between the two species of trees. Specifically speaking, we use a classical size-structured model, from which we derive a state-dependent delay differential equation, and we use this differential equation to fit the forest data from SORTIE. This differential equation is mathematically more tractable than the submodels in SORTIE.

In order to compare our mathematical model with SORTIE, we conduct numerical simulations and we get the best fit to the SORTIE forest data and the corresponding parameter values. One result we get is that the type of birth function of these two species is not of Ricker's type, as we have $\xi = 0$ in both best fits. We then extend our mathematical model to a two-species case with interspecific competition, and similarly we conduct the numerical comparison with SORTIE forest data, where we also get a very good fit.

Based on this, we go further and propose a model incorporating the spatial position parameter, to describe the density of population, or further, the number of population at every specific spatial position. We can see vividly the spread and succession in our numerical simulation. By using a spatial model, given the initial distribution we will be able to predict specifically the population at certain spatial position and time, which is more practical in reality. We refer to [9, 29] for more results about SORTIE model and spatially distributed forest.

We should mention that our model improves the computer simulator SORTIE from the following perspectives. First, in SORTIE model, every behaviour of each individual is described separately by a submodel which calculates specific relevant variables (for example, in the resource submodel, they calculate the light transmissivity through the crown and determine how much light is intercepted in each angle, which will be used in the growth submodel), and then all the behaviours are combined together to get the dynamics of the entire community. In our mathematical model, we simplify the above complicated processes of tree physiology by using only several functions instead to describe the mean behaviour of individuals, which is still effective. Thus there are fewer parameters to input in our mathematical model (8 parameters (or 4 more parameters in two-species model), while more than 20 parameters in SORTIE). This obviously makes it easier to operate the simulation. Second, the time it takes to run a simulation is much shorter due to the different computing mechanism. Thus, it's possible for us to explore the forest dynamics in a very long time scale. Third, the analysis of the mathematical model also permit us to study the coexistence of species in ecological time scale, which allows the maintenance of species diversity in nature. In our simulation, we reach a result that the population number of eastern hemlock decreases to 0 after a long enough time, which conforms to the competitive exclusion principle. However, by analyzing the existence of the interior coexistent equilibrium, we are able to establish a range of parameters in which the exclusion principle is no longer true. The coexistence result has also been confirmed by numerical simulations (with and without space). We refer to [1, 2, 5, 16, 17, 44] for more results going into that direction. But there are few results analyzing mathematically the coexistence for the solution of the structured model with partial differential equations (0.8). Also it is well known that light is a key influence in many forest systems [42], and our model can be used to reproduce the complicated mechanisms included into SORTIE model. But in reality, there are so many influencing factors, such as carbon, nitrogen, water, etc. [6, 18, 19, 22, 41], not only restricted to light. More work about these other influencing factors is left for future investigation.

Appendices

Appendix A Derivation of the state dependent FDE

The single species model (0.1) we consider here is very similar with the one considered by H. Smith in [37]. Nevertheless, our mortality rate $\mu(s)$ is dependent on the size s, so we will re-derive the state dependent FDE for completeness. Differentiating (0.4) with respect to t, we have

$$\begin{aligned}\frac{dA(t)}{dt} &= \int_{s^*}^{+\infty} \partial_t u(t,s)ds = -f(A(t)) \int_{s^*}^{+\infty} \partial_s u(t,s)ds - \int_{s^*}^{+\infty} \mu(s)u(t,s)ds \\ &= f(A(t))u(t,s^*) - \int_{s^*}^{+\infty} \mu(s)u(t,s)ds. \end{aligned} \tag{A.1}$$

Next we deal with the term $u(t,s^*)$. The characteristic curves for the first equation in (0.1) are (shown in Figure 13)

$$\frac{ds(t)}{dt} = f(A(t)). \tag{A.2}$$

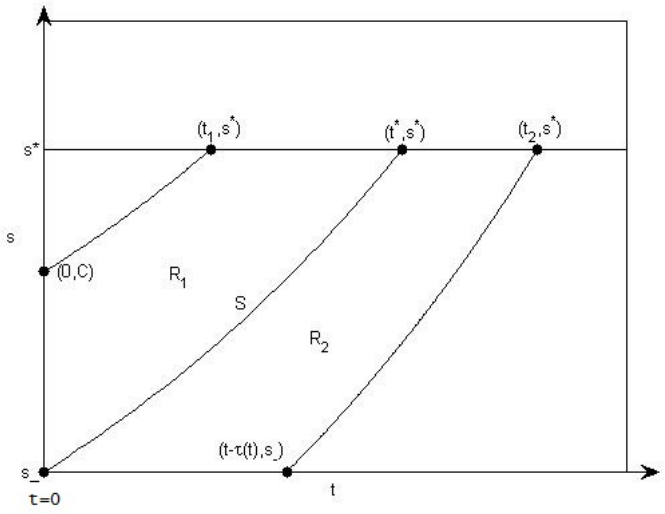

Figure 13: *In this figure we present the characteristic curves (A.2).*

Then we will have the following representation of s

$$C + \int_0^t f(A(\sigma))d\sigma = s(t). \tag{A.3}$$

Suppose t^* is the time when juveniles present at time 0 become adults, namely

$$\int_0^{t^*} f(A(\sigma))d\sigma = s^* - s_-. \tag{A.4}$$

We can see that the curve

$$S = \left\{(t,s) :\ 0 \leqslant t \leqslant t^*,\ s = s_- + \int_0^t f(A(\sigma))d\sigma\right\}$$

divides the strip $[0,+\infty) \times [s_-, s^*]$ into two parts R_1 and R_2. Assuming that $s - s_- \leqslant \int_0^t f(A(\sigma))d\sigma$, then we can find $T(t,s) \geqslant 0$ such that

$$\int_{t-T(t,s)}^t f(A(\sigma))d\sigma = s - s_- \tag{A.5}$$

in the region R_2, so it denotes the time it takes for a juvenile to grow to size s at time t from the minimal size s_-. Replacing s in $u(t,s)$ with (A.3), we can compute formally as follows, assuming that u is a C^1-function

$$\begin{aligned}
&\frac{d}{dt}u\left(t, C + \int_0^t f(A(\sigma))d\sigma\right)\\
=\ &\partial_t u\left(t, C + \int_0^t f(A(\sigma))d\sigma\right) + f(A(t))\partial_s u\left(t, C + \int_0^t f(A(\sigma))d\sigma\right)\\
=\ &-\mu\left(C + \int_0^t f(A(\sigma))d\sigma\right) u\left(t, C + \int_0^t f(A(\sigma))d\sigma\right).
\end{aligned}$$

This is a separable ODE with respect to t. Integration of this equation, and by using the initial distribution and the boundary condition, we obtain the following expression of $u(t,s)$

$$u(t,s) = \begin{cases} u_0\left(s - \int_0^t f(A(\sigma))d\sigma\right) e^{-\int_0^t \mu(s - \int_0^t f(A(\sigma))d\sigma + \int_0^l f(A(\sigma))d\sigma)dl}, \\ \qquad\qquad \text{if } s \geqslant s_- + \int_0^t f(A(\sigma))d\sigma, \\ \dfrac{\beta b(A(t - T(t,s)))}{f(A(t - T(t,s)))} e^{-\int_{t-T(t,s)}^t \mu(s_- + \int_{t-T(t,s)}^l f(A(\sigma))d\sigma)dl}, \\ \qquad\qquad \text{if } s \leqslant s_- + \int_0^t f(A(\sigma))d\sigma. \end{cases} \tag{A.6}$$

Whenever $s^* - s_- \leqslant \int_0^t f(A(\sigma))d\sigma$, we can specifically define $\tau(t) := T(t, s^*)$ as the solution of

$$\int_{t-\tau(t)}^{t} f(A(\sigma))d\sigma = s^* - s_-. \tag{A.7}$$

Actually the term $\tau(t) = T(t, s^*)$ represents the time spent by a newborn becoming an adult.

We now assume the mortality function as follows

$$\mu(s) = \begin{cases} \mu_A > 0, \text{ if } s \geqslant s^*, \\ \mu_J > 0, \text{ if } s \in [s_-, s^*). \end{cases}$$

Then when $s = s^*$, we have for $t \in [0, t^*]$,

$$u(t, s^*) = u_0 \left(s^* - \int_0^t f(A(\sigma))d\sigma \right) e^{-\mu_J t},$$

and for $t > t^*$,

$$u(t, s^*) = \frac{\beta b(A(t - \tau(t)))}{f(A(t - \tau(t)))} e^{-\mu_J \tau(t)}.$$

Replacing $u(t, s^*)$ back in (A.1), we get the model (0.5).

By differentiating the second equation of (0.5) in time, we obtain

$$\frac{d}{dt} \int_{t-\tau(t)}^{t} f(A(\sigma))d\sigma = 0 \Leftrightarrow f(A(t)) - f(A(t - \tau(t))) \left(1 - \tau'(t)\right) = 0.$$

Therefore the state-dependent delay differential equation (0.6) is derived.

Remark A.1 *Note that the function $t \to t - \tau(t)$ is strictly increasing because*

$$\frac{d}{dt} \left(t - \tau(t)\right) = \frac{f(A(t))}{f(A(t - \tau(t)))} > 0.$$

Remark A.2 *Notice that system (0.5) is valid when $t > t^*$. However, as this system is autonomous, we can make a translation so that the initial time of the system will become $t = 0$. But the numerical simulations are still conducted with the initial time $t = t^*$ for the sake of simplicity.*

We conduct a comparison between the growth function (0.2) and the intrinsic function of the growth submodel in the simulator SORTIE. From the model (0.3), we only care about the growth of juveniles, so first we assume the radius function of a juvenile

$$r(t) = \frac{\text{diam}_{10}(t)}{2}$$

where diam_{10} represents the diameter at 10cm height. We use the following change of variable to define the size s which we are using in the model (0.1)

$$s(t) := \ln \frac{r(t)}{r_-}, \tag{A.8}$$

where r_- is the minimal radius of the juvenile. We will have

$$s'(t) = \frac{r'(t)}{r(t)} = f(A(t)).$$

Then the approximation of the derivative of $r(t)$, which describes the growth of the radius, is

$$\frac{r(t+\Delta t) - r(t)}{\Delta t} = r(t) \cdot \frac{\alpha}{1+\delta A(t)} = r(t) \cdot \frac{\alpha A(t)^{-1}}{\delta + A(t)^{-1}}. \tag{A.9}$$

Take $\Delta t = 1$ (one year), then (A.9) shows the increase of the radius in one year.

On the other hand, we have the following formula for growth in SORTIE from [13, 27, 28]

$$\text{Annual Radius Increase} = \text{Radius} \cdot \frac{G_1 \cdot \text{GLI}}{\frac{G_1}{G_2} + \text{GLI}}, \tag{A.10}$$

where G_1 is the asymptotic growth rate at high light and G_2 is the slope at 0 or low light. The term GLI (global light index) describes the percentage of light transmitted through tree gaps and perceived by trees, thus is a measure for light. Comparing the two formulas (A.9) and (A.10), we find that they have the same form, and the parameters $A(t)^{-1}, \alpha, \delta$ correspond to GLI, $G_1, G_1/G_2$ respectively. So the choice of the growth function (0.2) is reasonable. Plus, this also explains what is size s in our model (0.1). By this definition of $s(t)$, we have the minimal size of juveniles $s_- = 0$ (as $r(t) = r_-$), and the minimal size of adults $s_* = \ln(r^*/r_-)$, where r^* is the minimal radius of adults.

Appendix B Positive equilibrium for two-species model

We compute the positive equilibrium for the system (0.9), which is, we compute the solution for the following equations

$$\begin{cases} 0 = e^{-\mu_{J_1}\tau_1}\beta_1 A_1 - \mu_{A_1} A_1, \\ \displaystyle\int_{t-\tau_1}^{t} \frac{\alpha_1}{1+\delta_1(\zeta_{11}A_1 + \zeta_{12}A_2)} d\sigma = s^* - s_-, \end{cases} \tag{B.1}$$

and

$$\begin{cases} 0 = e^{-\mu_{J_2}\tau_2}\beta_2 A_2 - \mu_{A_2} A_2, \\ \int_{t-\tau_2}^{t} \dfrac{\alpha_2}{1+\delta_2(\zeta_{21}A_1+\zeta_{22}A_2)} d\sigma = s^* - s_-, \end{cases} \tag{B.2}$$

Obviously, $A_1 = 0$, $A_2 = 0$ is a trivial equilibrium for the species, in which case we have

$$\tau_1 = \frac{s^* - s_-}{\alpha_1},\ \tau_2 = \frac{s^* - s_-}{\alpha_2}.$$

Moreover, we have two "boundary" equilibrium $(\bar{A}_1, 0)$ and $(0, \tilde{A}_2)$, where

$$\bar{A}_1 = \frac{1}{\delta_1\zeta_{11}}\left(\frac{\alpha_1}{\mu_{J_1}(s^*-s_-)}\ln\frac{\beta_1}{\mu_{A_1}} - 1\right),$$

$$\bar{\tau}_1 = \frac{1}{\mu_{J_1}}\ln\frac{\beta_1}{\mu_{A_1}},\ \bar{\tau}_2 = \frac{(s^*-s_-)(1+\delta_2\zeta_{21}\bar{A}_1)}{\alpha_2},$$

and

$$\tilde{A}_2 = \frac{1}{\delta_2\zeta_{22}}\left(\frac{\alpha_2}{\mu_{J_2}(s^*-s_-)}\ln\frac{\beta_2}{\mu_{A_2}} - 1\right),$$

$$\tilde{\tau}_1 = \frac{(s^*-s_-)(1+\delta_1\zeta_{12}\tilde{A}_2)}{\alpha_1},\ \tilde{\tau}_2 = \frac{1}{\mu_{J_2}}\ln\frac{\beta_2}{\mu_{A_2}}.$$

Now we turn to the positive equilibrium. As $A_1, A_2 \neq 0$, we solve the first equation in (B.1) and (B.2) and get

$$\tau_1 = \frac{1}{\mu_{J_1}}\ln\frac{\beta_1}{\mu_{A_1}},\quad \tau_2 = \frac{1}{\mu_{J_2}}\ln\frac{\beta_2}{\mu_{A_2}} \tag{B.3}$$

By the second equation of (B.1) and (B.2), we have

$$\begin{cases} \zeta_{11}A_1 + \zeta_{12}A_2 = \dfrac{1}{\delta_1}\left(\dfrac{\alpha_1\tau_1}{s^*-s_-} - 1\right), \\ \zeta_{21}A_1 + \zeta_{22}A_2 = \dfrac{1}{\delta_2}\left(\dfrac{\alpha_2\tau_2}{s^*-s_-} - 1\right) \end{cases} \tag{B.4}$$

We replace τ_1 and τ_2 in (B.4) by (B.3), and we get the following linear equations

$$\begin{cases} \zeta_{11}A_1 + \zeta_{12}A_2 = \Phi_1, \\ \zeta_{21}A_1 + \zeta_{22}A_2 = \Phi_2, \end{cases} \tag{B.5}$$

where

$$\Phi_1 := \frac{1}{\delta_1}\left[\frac{\alpha_1}{\mu_{J_1}(s^*-s_-)}\ln\frac{\beta_1}{\mu_{A_1}} - 1\right],\quad \Phi_2 := \frac{1}{\delta_2}\left[\frac{\alpha_2}{\mu_{J_2}(s^*-s_-)}\ln\frac{\beta_2}{\mu_{A_2}} - 1\right].$$

First, as we want a positive solution, we need the following conditions

$$\Phi_1 \geqslant 0,\ \Phi_2 \geqslant 0. \tag{B.6}$$

We solve the equation (B.5) directly without considering its solvability

$$A_1 = \frac{\zeta_{22}\Phi_1 - \zeta_{12}\Phi_2}{\zeta_{11}\zeta_{22} - \zeta_{12}\zeta_{21}}, \quad A_2 = \frac{\zeta_{11}\Phi_2 - \zeta_{21}\Phi_1}{\zeta_{11}\zeta_{22} - \zeta_{12}\zeta_{21}}. \tag{B.7}$$

In order to have a positive solution, we need the following conditions

$$\begin{cases} \zeta_{11}\zeta_{22} - \zeta_{12}\zeta_{21} > 0, \\ \zeta_{22}\Phi_1 - \zeta_{12}\Phi_2 > 0, \\ \zeta_{11}\Phi_2 - \zeta_{21}\Phi_1 > 0, \end{cases} \text{ or } \begin{cases} \zeta_{11}\zeta_{22} - \zeta_{12}\zeta_{21} < 0, \\ \zeta_{22}\Phi_1 - \zeta_{12}\Phi_2 < 0, \\ \zeta_{11}\Phi_2 - \zeta_{21}\Phi_1 < 0, \end{cases} \tag{B.8}$$

or in another simplified form

$$\frac{\zeta_{12}}{\zeta_{22}} < \frac{\Phi_1}{\Phi_2} < \frac{\zeta_{11}}{\zeta_{21}}, \quad \text{or} \quad \frac{\zeta_{11}}{\zeta_{21}} < \frac{\Phi_1}{\Phi_2} < \frac{\zeta_{12}}{\zeta_{22}}, \tag{B.9}$$

So we have

Lemma B.1 *Under the condition* (B.6) *and* (B.9)*, the equations* (B.1) *and* (B.2) *have a positive equilibrium as in* (B.7).

We check the conditions (B.6) and (B.9) for our previous results in Table 1-3, and we have

$$\Phi_1 = 100.6839 > 0, \quad \Psi_2 = 133.4324 > 0,$$

$$\frac{\zeta_{12}}{\zeta_{22}} = 0.6, \quad \frac{\Phi_1}{\Phi_2} = 0.7546, \quad \frac{\zeta_{11}}{\zeta_{21}} = 0.625,$$

which does not satisfy the condition (B.9), so there is no positive equilibrium in our previous simulation, and eastern hemlock is disappearing. In order to have a positive equilibrium, we reduce the influence of American beech towards eastern hemlock, namely we lower ζ_{21} from 1.6 to 1. Then we have

$$\frac{\zeta_{11}}{\zeta_{21}} = 1,$$

which satisfies the condition (B.9). And we have the coexistence of both species as is shown in Figure 8 and Figure 12.

Appendix C Resolvent of the Laplacian operator Δ

Assume that $\psi(x,y) : [0, x_{\max}] \times [0, y_{\max}] \to \mathbb{R}$ is a function. The resolvent of the Laplacian operator Δ with periodic boundary condition is given for $(x,y) \in [0, x_{\max}] \times [0, y_{\max}]$ by

$$(\lambda I - \varepsilon\Delta)^{-1}(\psi)(x,y) = \int_0^{+\infty} e^{-\lambda t} T_\Delta(\varepsilon t)(\widehat{\psi})(x,y)dt, \tag{C.1}$$

where $\widehat{\psi}$ extends ψ periodically on $\mathbb{R} \times \mathbb{R}$, that is to say

$$\widehat{\psi}(x,y) = \psi(x,y), \forall (x,y) \in [0, x_{\max}] \times [0, y_{\max}]$$

and

$$\begin{cases} \widehat{\psi}(x + x_{\max}, y) = \widehat{\psi}(x,y), \forall x, y \in \mathbb{R}, \\ \widehat{\psi}(x, y + y_{\max}) = \widehat{\psi}(x,y), \forall x, y \in \mathbb{R}. \end{cases}$$

Moreover $T_\Delta(t)$ is the semigroup generated by the Laplacian operator Δ. A result in Engel and Nagel [11, p. 69] shows that

$$T_\Delta(t)(\widehat{\psi})(x,y) = \frac{1}{4\pi t} \iint_{\mathbb{R}^2} e^{-\frac{(x-\widehat{x})^2 + (y-\widehat{y})^2}{4t}} \widehat{\psi}(\widehat{x}, \widehat{y}) d\widehat{x} d\widehat{y}. \tag{C.2}$$

The numerical approximation of $(I - \varepsilon_i\Delta)^{-1}$ is given by the matrix $(I + \varepsilon_i \mathbf{A})^{-1}$ where

$$\mathbf{A} = \begin{pmatrix} \mathbf{B} & \mathbf{C} & 0 & ... & \mathbf{C} \\ \mathbf{C} & \mathbf{B} & \ddots & \ddots & \vdots \\ 0 & \ddots & \ddots & \ddots & 0 \\ \vdots & \ddots & \ddots & \ddots & \mathbf{C} \\ \mathbf{C} & ... & 0 & \mathbf{C} & \mathbf{B} \end{pmatrix},$$

where

$$\mathbf{B} = \begin{pmatrix} \frac{2}{dx^2} + \frac{2}{dy^2} & -\frac{1}{dx^2} & 0 & ... & ... & -\frac{1}{dx^2} \\ -\frac{1}{dx^2} & \frac{2}{dx^2} + \frac{2}{dy^2} & -\frac{1}{dx^2} & \ddots & & \vdots \\ 0 & \ddots & \ddots & \ddots & \ddots & \vdots \\ \vdots & \ddots & \ddots & \ddots & \ddots & 0 \\ \vdots & & \ddots & \ddots & \ddots & -\frac{1}{dx^2} \\ -\frac{1}{dx^2} & ... & ... & 0 & -\frac{1}{dx^2} & \frac{2}{dx^2} + \frac{2}{dy^2} \end{pmatrix}$$

and

$$\mathbf{C} = \begin{pmatrix} -\frac{1}{dy^2} & 0 & ... & 0 \\ 0 & \ddots & \ddots & \vdots \\ \vdots & \ddots & \ddots & 0 \\ 0 & ... & 0 & -\frac{1}{dy^2} \end{pmatrix}.$$

References

[1] T. P. Adams, D. W. Purves, and S. W. Pacala. Understanding height-structured competition in forests: is there an R^* for light? Proceedings of the Royal Society B, 274:3039–3048, 2007.

[2] Ó. Angulo, R. B. de la Parra, J. C. López-Marcos, and M. A. Zavala. Stand dynamics and tree coexistence in an analytical structured model: The role of recruitment. Journal of Theoretical Biology, 333:91–101, 2013.

[3] D. B. Botkin. Forest dynamics: An ecological model. Oxford University Press, 1993.

[4] D. B. Botkin, J. F. Janak, and J. R. Wallis. Some ecological consequences of a computer model of forest growth. Journal of Ecology, 60:849–872, 1972.

[5] M. Cammarano. Co-dominance and succession in forest dynamics: The role of interspecific differences in crown transmissivity. Journal of Theoretical Biology, 285:46–57, 2011.

[6] A. Cheaïb, A. Mollier, S. Thunot, C. Lambrot, S. Pellerin, and D. Loustau. Interactive effects of phosphorus and light availability on early growth of maritime pine seedlings. Annals of Forest Science, 62:575–583, 2005.

[7] A. M. de Roos and L. Persson. Competition in size-structured populations: mechanisms inducing cohort formation and population cycles. Theoretical Population Biology, 63:1–16, 2003.

[8] P. A. Delcourt and H. R. Delcourt. Long-term forest dynamics of the temperate zone: A case study of late-quaternary forests in eastern North America. Springer New York, 1987.

[9] D. H. Deutschman, S. A. Levin, and S. W. Pacala. Error propagation in a forest succession model: the role of fine-scale heterogeneity in light. Ecology, 80(6):1927–1943, 1999.

[10] A. Ducrot. Travelling waves for a size and space structured model in population dynamics: Point to sustained oscillating solution connections. Journal of Differential Equations, 250:410–449, 2011.

[11] K. J. Engel and R. Nagel. One-parameter semigroups for linear evolution equations. Springer Science & Business Media, 1999.

[12] D. S. Falster, Å. Brännström, U. Dieckmann, and M. Westoby. Influence of four major plant traits on average height, leaf-area cover, net primary productivity, and biomass density in single-species forests: a theoretical investigation. Journal of Ecology, 99:148–164, 2011.

[13] R. K. Kobe, S. W. Pacala, J. A. Silander Jr., and C. D. Canham. Juvenile tree survivorship as a component of shade tolerance. Ecological Applications, 5(2):517–532, 1995.

[14] P. Köhler and A. Huth. An individual based rain forest model - concepts and simulation results. In A. Kastner-Maresch, W. Kurth, M. Sonntag, and B. Breckling, editors, Individual-based structural and functional models in ecology, volume 52 of Bayreuther Forum Ökologie, pages 35–51. Bayreuther Institut für terrestrische Ökosystemforschung, Bayreuth, 1998.

[15] T. Kohyama. Size-structured tree populations in gap-dynamic forest – the forest architecture hypothesis for the stable coexistence of species. Journal of Ecology, 81:131–143, 1993.

[16] T. Kohyama and T. Takada. The stratification theory for plant coexistence promoted by one-sided competition. Journal of Ecology, 97:463–471, 2009.

[17] T. S. Kohyama and T. Takada. One-sided competition for light promotes coexistence of forest trees that share the same adult height. Journal of Ecology, 100:1501–1511, 2012.

[18] T. E. Kolb, K. C. Steiner, L. H. McCormick, and T. W. Bowersox. Growth response of northern red-oak and yellow-poplar seedlings to light, soil moisture and nutrients in relation to ecological strategy. Forest Ecology and Management, 38:65–78, 1990.

[19] K. Kramer, I. Leinonen, and D. Loustau. The importance of phenology for the evaluation of impact of climate change on growth of boreal, temperate and mediterranean forests ecosystems: an overview. International Journal of Biometeorology, 44:67–75, 2000.

[20] S. A. Levin, B. Grenfell, A. Hastings, and A. S. Perelson. Mathematical and computational challenges in population biology and ecosystems science. Science, 275:334–343, 1997.

[21] J. Liu and P. S. Ashton. Individual-based simulation models for forest succession and management. Forest Ecology and Management, 73:157–175, 1995.

[22] D. Loustau, S. Crepeau, M. G. Guye, M. Sartore, and E. Saur. Growth and water relations of three geographically separate origins of maritime pine (pinus pinaster) under saline conditions. Tree Physiology, 15:569–576, 1995.

[23] P. Magal and S. Ruan. Center manifolds for semilinear equations with non-dense domain and applications to hopf bifurcation in age structured models. In AMS eBook Collections, volume 202 of Memoirs of the American Mathematical Society. American Mathematical Society, Providence, Rhode Island, 2009.

[24] P. Magal and Z. Zhang. State-dependent delay differential equation modelling forest growth I: semiflow properties *(in preparation)*.

[25] N. L. E. Obiang, A. Ngomanda, O. Hymas, É. Chézeauxl, and N. Picard. Diagnosing the demographic balance of two light-demanding tree species populations in central africa from their diameter distribution. Forest Ecology and Management, 313:55–62, 2014.

[26] C. D. Oliver and B. C. Larson. Forest stand dynamics. McGraw-Hill Inc., 1990.

[27] S. W. Pacala, C. D. Canham, J. Saponara, J. A. Silander Jr., R. K. Kobe, and E. Ribbens. Forest models defined by field measurements: estimation, error analysis and dynamics. Ecological Monographs, 66(1):1–43, 1996.

[28] S. W. Pacala, C. D. Canham, and J. A. Silander Jr. Forest models defined by field measurements: I. the design of a northeastern forest simulator. Canadian Journal of Forest Research, 23:1980–1988, 1993.

[29] S. W. Pacala, C. D. Canham, J. A. Silander Jr., and R. K. Kobe. Sapling growth as a function of resources in a north temperate forest. Canadian Journal of Forest Research, 24:2172–2183, 1994.

[30] A. Porté and H. H. Bartelink. Modelling mixed forest growth: a review of models for forest management. Ecological Modelling, 150:141–188, 2002.

[31] H. Pretzsch. Forest dynamics, growth and yield: From measurement to model. Springer Berlin Heidelberg, 2009.

[32] E. Ribbens, J. A. Silander Jr., and S. W. Pacala. Seedling recruitment in forests: calibrating models to predict patterns of tree seedling dispersion. Ecology, 75(6):1794–1806, 1994.

[33] W. E. Ricker. Stock and recruitment. Journal of the Fisheries Research Board of Canada, 11(5):559–623, 1954.

[34] W. E. Ricker. Computation and interpretation of biological studies of fish populations. In Bulletin of the Fisheries Research Board of Canada, volume 191. Fisheries and Marine Service, Ottawa, 1975.

[35] H. H. Shugart and D. C. West. Development of an appalachian deciduous forest succession model and its application to assessment of the impact of the chestnut blight. Journal of Environmental Management, 5:161–179, 1977.

[36] H. H. Shugart. A theory of forest dynamics: The ecological implications of forest succession models. Springer-Verlag New York, 1984.

[37] H. L. Smith. Reduction of structured population models to threshold-type delay equations and functional differential equations: a case study. Mathematical Biosciences, 113:1–23, 1993.

[38] H. L. Smith. A structured population model and a related functional differential equation: global attractors and uniform persistence. Journal of Dynamics and Differential Equations, 6(1):71–99, 1994.

[39] N. Strigul, D. Pristinski, D. Purves, J. Dushoff, and S. Pacala. Scaling from trees to forests: tractable macroscopic equations for forest dynamics. Ecological Monographs, 78(4):523–545, 2008.

[40] R. M. Teck and D. E. Hilt. Individual-tree diameter growth model for the northeastern united states. Research paper NE-649, US. Department of Agriculture, Forest Service, Northeastern Forest Experiment Station, Radnor, PA, 1991.

[41] P. Trichet, D. Loustau, C. Lambrot, and S. Linder. Manipulating nutrient and water availability in a maritime pine plantation: effects on growth, production, and biomass allocation at canopy closure. Annals of Forest Science, 65(8):814, 2008.

[42] F. Valladares and Ü. Niinemets. Shade tolerance, a key plant feature of complex nature and consequences. Annual Review of Ecology, Evolution, and Systematics, 39:237–257, 2008.

[43] M. Yokozawa and T. Hara. Foliage profile, size structure and stem diameter-plant height crowded plant populations. Annals of Botany, 76:271–285, 1995.

[44] M. A. Zavala, Ó. Angulo, R. B. de la Parra, and J. C. López-Marcos. An analytical model of stand dynamics as a function of tree growth, mortality and recruitment: The shade tolerance-stand structure hypothesis revisited. Journal of Theoretical Biology, 244:440–450, 2007.

Tables

Parameter	Interpretation	value	Reference
μ_{J_1}	natural mortality rate for juveniles	0.03	estimated
μ_{A_1}	natural mortality rate for adults	0.001	estimated
β_1	birth rate in absence of birth limitation	2	estimated
s_-	minimal size for juvenile	0	[28]
s^*	minimal size for adult	$\ln 50$	[32]
ξ_1	parameter in the Ricker type function	0	estimated
τ_{01}	time delay of the juveniles present	121	estimated
	at time 0 to become adults		
α_1	growth rate of juveniles without adults	0.1709	computed
δ_1	parameter describing the descending speed		
	of the growth ratewhen adult population increases	0.1	estimated

Table 1: Parameter values of the best fit for species 1: American beech.

Parameter	Interpretation	value	Reference
μ_{J_2}	natural mortality rate for juveniles	0.031	estimated
μ_{A_2}	natural mortality rate for adults	0.0037	estimated
β_2	birth rate in absence of birth limitation	4	estimated
s_-	minimal size for juvenile	0	[28]
s^*	minimal size for adult	$\ln 50$	[32]
ξ_2	parameter in the Ricker type function	0	estimated
τ_{02}	time delay of the juveniles present at time 0 to become adults	127	estimated
α_2	growth rate of juveniles without adults	0.249	computed
δ_2	parameter describing the descending speed of the growth rate when adult population increases	0.1	estimated

Table 2: Parameter values of the best fit for species 2: eastern hemlock.

Parameter	Interpretation	value	Reference
ζ_{11}	parameter in the competition term describing the intraspecific competition among American beech	1	estimated
ζ_{12}	parameter in the competition term describing the interspecific influence of eastern hemlock on American beech	0.6	estimated
ζ_{21}	parameter in the competition term describing the interspecific influence of American beech on eastern hemlock	1.6	estimated
ζ_{22}	parameter in the competition term describing the intraspecific competition among eastern hemlock	1	estimated
τ_{01}	time delay of the American beech juveniles present at time 0 to become adults	201	estimated
τ_{02}	time delay of the eastern hemlock juveniles present at time 0 to become adults	208	estimated

Table 3: Other parameter values for two-species model.